Article

A Cascade Chromogenic System with Exponential Signal Amplification for Visual Colorimetric Detection of Acetone

Jingkai Liang, Hua Li, Junren Wang, Haili Yu, and Yi He

Anal. Chem., **Just Accepted Manuscript** • Publication Date (Web): 14 Apr 2020

A Cascade Chromogenic System with Exponential Signal Amplification for Visual Colorimetric Detection of Acetone

Jingkai Liang[+ a], Hua Li[+b], Junren Wang [a], Haili Yu [a], Yi He[* a]

a National Collaborative Innovation Center for Nuclear Waste and Environmental Safety, School of National Defence Science & Technology, Southwest University of Science and Technology, Mianyang 621010, P. R. China.

b SUSTech Core Research Facilities, Southern University of Science and Technology, Shenzhen 518055, China.

[+]These authors contributed equally.

*Corresponding author: Prof. Dr. Yi He, Tel: +86-816-6089885, Fax: +86-816-6089889, Email: yhe2014@126.com.

ABSTRACT: The signal of the traditional chromogenic systems is directly proportional to analyte concentration, leading to an unsatisfactory sensitivity. Herein, we report a cascade chromogenic system to realizing exponential amplification of colorimetric signal through coupling chemical oxidation with photo-induced radical chain reaction. The chemical oxidation of *o*-phenylenediamine (OPD) by Fe^{3+} generates Fe^{2+} and photoactive 2,3-diaminophenazine (DAP), Under blue light irradiation, DAP initiates the formation of holes and H_2O_2 that reacts with Fe^{2+} to hydroxyl radicals (·OH) and Fe^{3+} via an intersystem crossing (ISC) process. Moreover, the holes oxidize water to yield ·OH as well. The resulting ·OH and re-generated Fe^{3+} in turn oxidize OPD to yield more DAP, leading to a self-propagating reaction cycle that continues to proceed until all the OPD molecules are consumed, along with a distinct color change from colorless to yellow. Through the generation of the complex between DAP and acetone that limits the ISC process and therefore quenches the colorimetric signal, the highly sensitive and selective naked-eye detection of acetone is achieved from 50 μM to 3 mM, with a limit of detection of 35 μM. Additionally, the feasibility of this colorimetric assay to detect acetone in real water samples is also demonstrated.

KEYWORDS: Cascade chromogenic system, exponential amplification, colorimetric detection, acetone, *o*-phenylenediamine

INTRODUCTION

Colorimetric assays have been received a great research interest because of their simple operation, portable device, low cost, and convenient readout with the naked eyes[1-3]. These characteristics enable various colorimetric assays extremely for in-field detection of several target analytes, especially in resource-limited region[4-6]. To date, various chromogenic systems such as enzyme-catalyzed chromogenic reactions and plasmonic nanomaterials (gold, silver and highly doped semiconductors) have been employed for visual colorimetric analysis[6-11]. However, the absorbance signal of these systems is directly proportional to the concentration of analytes, resulting in a relatively low sensitivity and narrow dynamic range[12, 13]. In order to increase the colorimetric response to an analyte, exponential amplification methods have been utilized, including polymerase chain reaction (PCR) and dendritic chain reaction (DCR)[13-16]. Nevertheless, the reported exponential amplification protocols rely on enzymes or auto-inductive molecular receptors which require tedious and laborious multiple organic preparation procedure.

On the other hand, the reported exponential amplification methods are limited to the detection of fluoride ions, hydrogen peroxide, Pd(II), and nerve agents[17-23]. Other analytes such as acetone is not realized. As a common organic solvent, acetone is highly volatile, and it may damage human brain, kidney, and liver[24]. Traditional analytical techniques for detection of acetone, such as electrochemistry, chromatography, mass spectroscopy, are expensive, time-consuming or high detection temperature[25]. On the contrary, visual colorimetric methods are facile, rapid and cost-effective. Accordingly, it is vital to develop reliable, highly selective and sensitive colorimetric assays for acetone.

In this work, we propose a cascade chromogenic system based on coupling chemical oxidation with photo-induced radical chain reaction for highly sensitive and selective detection of acetone. Figure 1 shows the principle of the colorimetric assay for acetone. The oxidation-sensitive *o*-phenylenediamine (OPD) is selected as the chromogenic substrate. When the ferric ion (Fe^{3+}) as oxidant is introduced to the OPD solution, the

redox reaction between Fe^{3+} and OPD occurs to yield Fe^{2+} and 2,3-diaminophenazine (DAP) (Figure 1a).

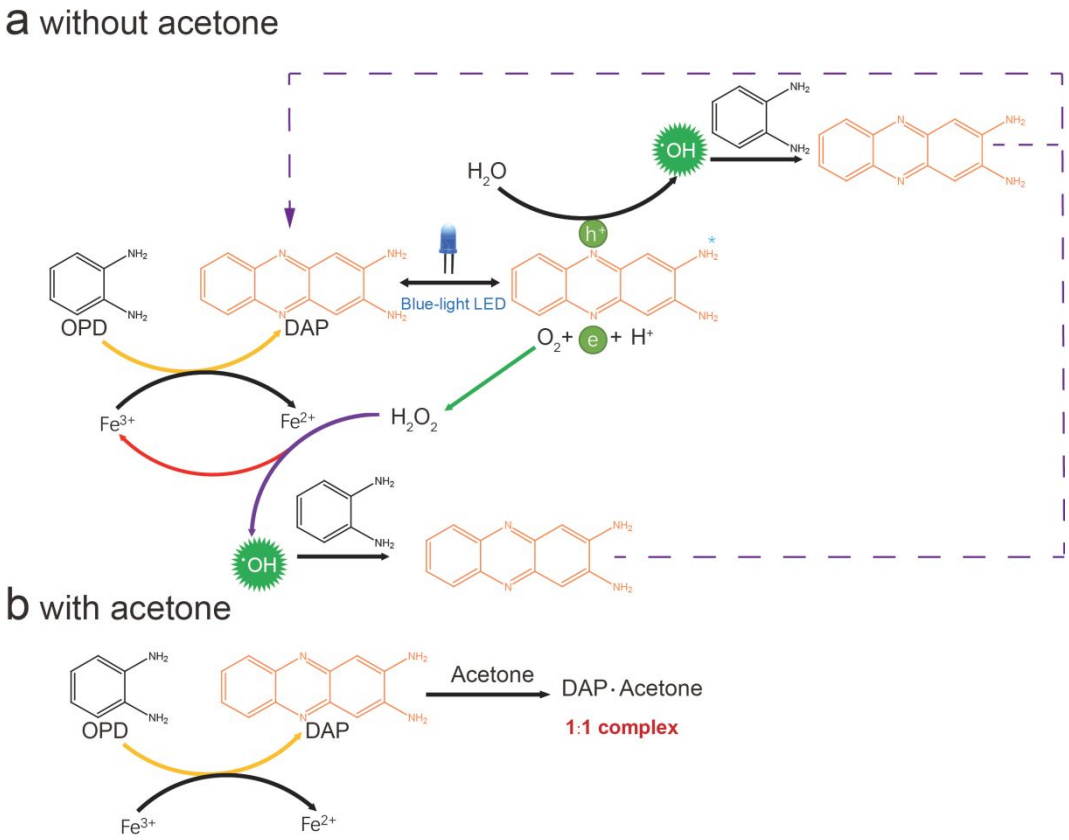

Figure 1. Schematic illustration of the cascade chromogenic system based on coupling chemical oxidation with photo-induced radical chain reaction for visual colorimetric detection of acetone.

Under blue light irradiation, DAP is excited after absorption of photons. The electrons are transited to higher-energy singlet orbitals (S_1) that are further transited to lower-energy triplet excited states (T_1) via an intersystem crossing (ISC) process due to the presence of a small singlet-triplet energy gap (ΔE_{ST}), along with the formation of the holes (Figure 1a). After that, the excited electrons react with dissolved oxygen to produce H_2O_2 in an acidic medium. Subsequently, the Fenton reaction of Fe^{2+} and H_2O_2 proceeds to yield hydroxyl radicals (·OH) and Fe^{3+} (Figure 1a). Moreover, the holes can directly oxidize water to generate ·OH as well. The re-generated Fe^{3+} and ·OH can oxidize OPD to create more DAP. The oxidation process of OPD progresses exponentially until all of the OPD are oxidized under an ideal condition. The cascade

chromogenic system is able to be monitored by the UV-vis absorption spectra of yellow DAP solution. In contrast, when acetone is added to the cascade chromogenic system, the complex of DAP and acetone with a molar ratio of 1:1 is engendered (Figure 1b). The resulting molecular complex gives a large increase in the value of ΔE_{ST}, which restrains ISC process and the photo-induced radical chain reaction and thus less DAP is produced. Through the change of the UV-vis absorption spectra of this chromogenic system, visual and quantitative analysis of acetone can be performed in water. Meanwhile, the colorimetric assay is further applied to analyze diluted real water samples.

EXPERIMENTAL SECTION

Materials. OPD, ferrous(III) chloride hexahydrate ($FeCl_3 \cdot 6H_2O$), ferrous chloride tetrahydrate ($FeCl_2 \cdot 4H_2O$), acetone, 1,10-phenanthroline, sulphuric acid (H_2SO_4), and methanol were purchased from Aladdin Chemical Reagent Co., Ltd (Shanghai, China). 5,5-dimethyl-1-pyrroline N-oxide (DMPO), sodium hydroxide (NaOH), ethanol, isopropanol, glycerol, ethyl acetate, ethylenediamine, dimethyl sulfoxide, methyl methacrylate, N-methyl pyrrolidone, diethylene glycol, ethylene acetate, sodium carbonate (Na_2CO_3), and other inorganic salts were obtained from ChengDu KeLong Chemical Co., Ltd (Chendu, China). All the reagents were of analytical grade and used as received. Deionized water was applied to prepare various solutions.

Procedure for Monitoring the Chromogenic System. Briefly, 0.3 mL of 1 mM OPD aqueous solution was added to a 0.25 mL of 0.6 mM $FeCl_3$ solution. Subsequently, the pH of the mixture solution was adjusted to 4.5 by using 0.1 M H_2SO_4. Then, the resulting solution was further diluted with deionized water, and a final reaction volume was maintained at 3 mL, followed by illumination with blue light-emitting diode (LED, 12 W) for 15 min at room temperature (approximatively 25°C). The UV-vis absorption spectra were acquired by a UV-vis photometer, and the corresponding optical images were collected by a digital camera. In order to evaluate the related reaction conditions, including pH, Fe^{3+} concentration, and LEDs of various colors, a similar experimental operation was carried out.

Procedure for Visual Colorimetric Determination of Acetone. To a 5 mL of glass bottle, 0.3 mL of 1 mM OPD aqueous solution, 0.25 mL of 0.6 mM Fe^{3+}, and 0.3 mL acetone with different concentrations were sequentially added; the pH of this mixture was adjusted to 4.5, followed by dilution to 3 mL with deionized water. After illumination with blue light-LED for 15 min at room temperature, the UV-vis absorption spectra of the mixture solution and optical images were collected. In order to investigate the selectivity of this colorimetric assay, acetone was replaced by other common solvents, and the same experimental operations were conducted.

Procedure for Acetone in Spiked Real Water. Three types of real water such as lake water, river water, and pond water were collected from Mianyang (China). These real water samples were filtered and diluted 50 times with deionized water. Then, the diluted water samples were spiked with 0.05, 0.4, and 2 mM of acetone, and the spiked samples were determined by the present colorimetric assay.

Characterization. Ultraviolet-visible (UV-vis) absorption spectra were acquired by an UV-1800 spectrophotometer. Electron paramagnetic resonance (EPR) spectra were performed at 298 K on a Bruker I200 EPR spectrometer equipped with a blue-light LED. Mass spectra were collected from a Q-Exactive high-resolution mass spectrometer. Fluorescence measurements were performed with the F-7000 fluorescent spectrophotometer.

RESULTS AND DISCUSSION

Exponential Amplification Chromogenic System. In order to examine the cascade chromogenic system based on coupling chemical oxidation with photo-induced radical chain reaction, 0.1 mM OPD solution is incubated with 50 μM Fe^{3+} under blue-light LED illumination for 15 min. As we expected, the chromogenic system with a yellow color shows a strong optical absorption in the visible region, and the maximum absorption peak is found at 446 nm (Figure 2a, curve iv), which is the characteristic absorption band of DAP[26-29]. Moreover, the production of DAP is further demonstrated by mass spectroscopy, and its molecular ion peak at 211. 0972 is clearly seen in the Figure S1. In contrast, the mixture of 50 μM Fe^{3+} and 0.1 mM OPD without

blue-light LED illumination displays a weak absorption (Figure 2a, curve iii), suggesting that the chemical oxidation reaction between Fe^{3+} and OPD can not effectively generate optical absorption because of the lack of enough DAP molecules in the solution.

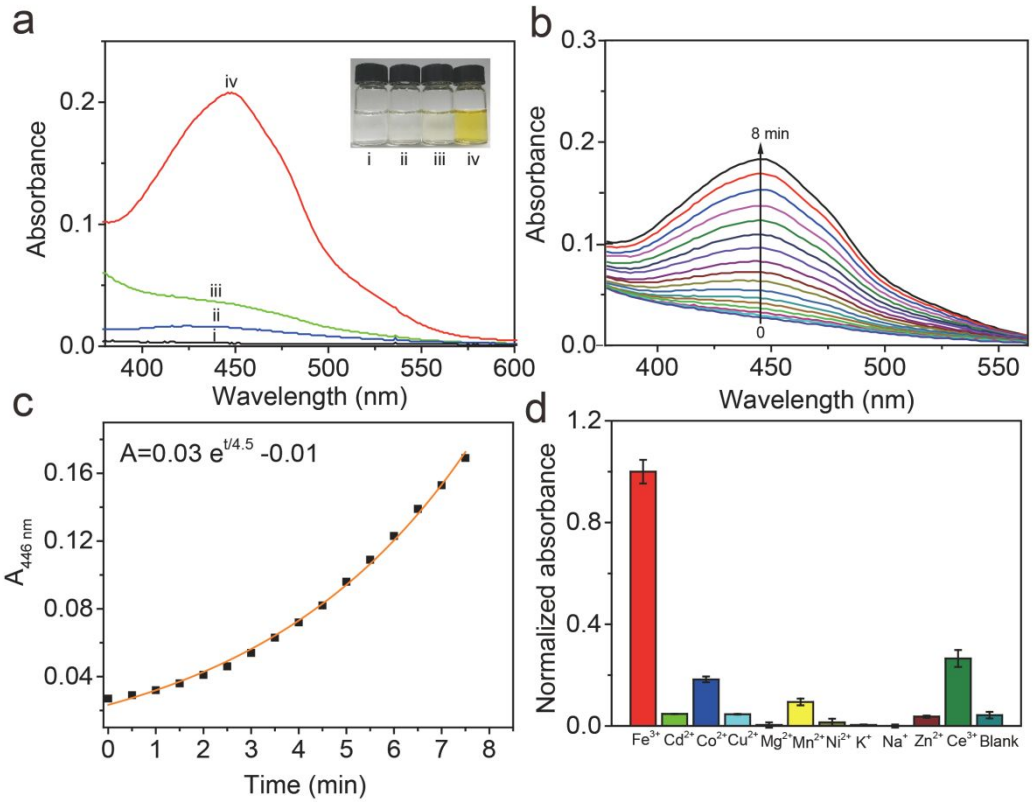

Figure 2. OPD oxidation-involved chromogenic reaction. (a) UV-vis absorption spectra of 0.1 mM OPD solution under different reaction conditions: i) in the dark, ii) blue-light LED illumination for 15 min, iii) reaction with 0.05 mM Fe^{3+} in the dark and iv) under blue-light LED illumination. (b) Time-dependent UV-vis absorption spectra for the chromogenic system. (c) Exponential relationship between reaction time and absorbance values of the chromogenic system at 446 nm. (d) Effect of several metal ions on the chromogenic system. The concentration of all the metal ions is 50 μM.

Similarly, direct blue-light illumination of OPD solution at a low concentration (0.1 mM OPD) is unable to induce the chromogenic phenomenon (Figure 2a, curve ii). The corresponding absorbance value of the cascade chromogenic system at 446 nm is 5.9 times and 13 times higher than those of Fe^{3+}-triggered chemical oxidation and direct

blue light-induced oxidation of OPD, respectively. It should be noted that when the OPD concentration is higher than 5 mM, direct blue-light illumination can induce the OPD oxidation because partial OPD is oxidized by dissolved oxygen to yield DAP that autocatalytically oxidize OPD[30].

To confirm the exponential amplification of colorimetric signal, the kinetic curves of the chromogenic system are collected as shown in Figure 2b. It can be seen that the DAP is formed with an exponentially increasing rate under illumination with blue light. The absorbance data in Figure 2c fit well to the exponential progress curve, demonstrating the exponential signal behavior of this chromogenic system. In addition, some experimental conditions such as pH and Fe^{3+} concentration are capable of influencing this chromogenic system. As shown in Figure S2, the optimized pH is found to be 4.5. The reason is that Fe^{3+} is easily hydrolyzed at a high pH, and OPD will be completely protonated under a strong acidic medium, which is adverse to the photochemical oxidation of OPD. Figure S3 shows the effect of Fe^{3+} concentration on the absorbance value of this chromogenic reaction. When the concentration of Fe^{3+} is more than 50 μM, the absorbance tends to reach a saturation value. Therefore, 50 μM Fe^{3+} is utilized in the exponential amplification chromogenic system. Except for Fe^{3+}, other common metal ions such as Cd^{2+}, Co^{2+}, Cu^{2+}, Mg^{2+}, Mn^{2+}, Ni^{2+}, K^{+}, Na^{+}, Zn^{2+}, and Ce^{3+} can not exhibit an obvious signal enhancement (Figure 2d). Although Ce^{3+} has a certain capacity for oxidation of OPD, the reduction product (Ce^{2+}) may not be able to initiate the Fenton reaction. Accordingly, the cascade reaction between Fe^{3+}-induced chemical oxidation and photo-induced radical chain produces an exponential amplification chromogenic system.

Identification of Chromogenic Reaction Mechanism. To thoroughly identify the reaction mechanism of the cascade chromogenic system, we firstly illuminate the mixture of Fe^{3+} and OPD with red, green, and blue LED. We find the generation of the strong absorbance signal only under blue-light illumination (λ_{max}= 454 nm) (Figure 3a and Figure S4), which overlaps well with the absorption of DAP (λ_{max}= 446 nm). To confirm the fact that DAP can be photo-excited, the fluorescent emission spectra of DAP solution is collected with a 445 nm-excitation wavelength. A significant emission

peak is observed at 564 nm (Figure S5), demonstrating that the excited-state DAP (DAP*) will be created under blue-light LED illumination.

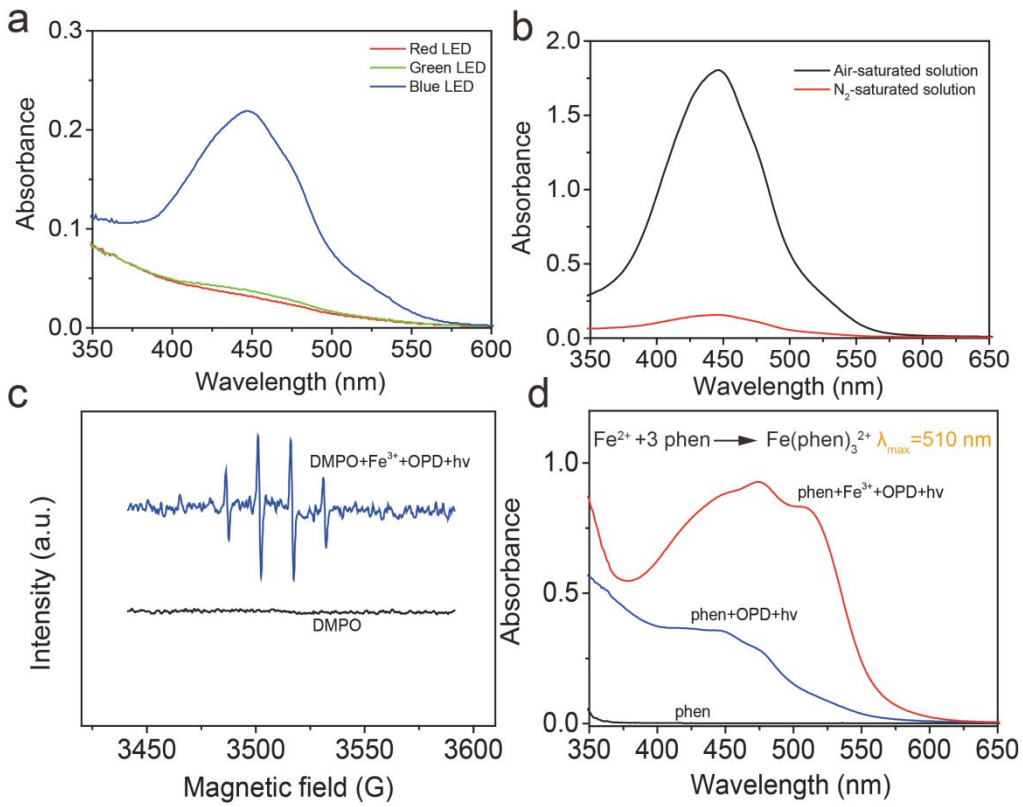

Figure 3. Reaction mechanism. (a) UV-vis absorption spectra of the exponential amplification chromogenic system under irritation with different colors of LED for 15 min. The light power density of blue, green, and red LED is about 48 mW cm^{-2}. (b) Effect of reaction atmosphere on the chromogenic system. (c) Electron paramagnetic resonance spectra of DMPO and the mixture of DMPO, Fe^{3+} and OPD under irradiation with blue-light LED. (d) UV-vis absorption spectra of 0.5 mM 1,10-phenanthroline and the mixture of 0.5 mM 1,10-phenanthroline (phen) and OPD in the absence and presence of 0.4 mM Fe^{3+}. The inset shows the coordination reaction of phen with Fe^{2+}.

According to the reaction principle of the cascade chromogenic system (Figure 1), the production of H_2O_2 as an important transient intermediate is directly dependent on the concentration of dissolved oxygen. To confirm this reaction pathway, the role of dissolved oxygen is examined. When the nitrogen gas is bubbled into the chromogenic system, the absorbance value at 446 nm remarkably decreases up to 92% (Figure 3b), indirectly support the formation of transient H_2O_2.

After affirming the role of dissolve oxygen, we then investigate the reactive oxygen species (ROS) with ROS scavengers, including ascorbic acid for all the ROS[31], thiourea, NaN_3 as well as Na_2CO_3 that are served as scavengers of ·OH, $^1O_2$, and $^{\cdot-}O_2$[32-35], respectively (Figure S6-Figure S9). Only ascorbic acid and thiourea are in a position to quench the cascade chromogenic reaction. Besides, the type of ROS is also studied by EPR spectroscopy using 5,5-dimethyl-1-pyrroline N-oxide (DMPO) as the ROS probe. The characteristic quadruplet peak from the spin-adduct of DMPO and ·OH with a 1:2:2:1 intensity is obtained as illustrated in Figure 3c. These results clearly demonstrate that the ·OH is the key intermediate in the cascade chromogenic system[36]. Additionally, the existence of Fe^{2+} is verified by introducing 1,10-phenanthroline (phen) as the ligand for Fe^{2+}. As indicated in Figure 3d, there is an absorption peak at 510 nm, which is attributed to the absorption feature of $Fe(phen)_3^{2+}$ complex[37, 38]. Based on these results, the chromogenic reaction mechanism in Figure 1 is well certified.

Acetone-Response Behavior and Visual Quantitative Detection of Acetone. Next, the acetone-response behavior of this cascade chromogenic system is further explored. As displayed in Figure 4a, the addition of acetone results in a distinct quenching for the absorbance in the visible region, and only background signal from the optical absorption of Fe^{3+} is gained, accompanying a color change from yellow to colorless. In order to appraise the reaction product in the presence of acetone, a high-resolution mass spectrometer is conducted. The molecular ion peak at 269.13876 is ascribed to the complex of DAP and acetone with a molar ratio of 1:1 (Figure S10), revealing that the generation of DAP · acetone complex inhibits the chromogenic reaction. Furthermore, the interaction of DAP and acetone in the complex is calculated according to the B3LYP with 6-31G basis set based on the time-dependent density functional theory (TD-DFT) approach, which is analyzed by Multiwfn software[39]. The calculated interaction force between DAP and acetone is mainly consisting of hydrogen bonds and Van der Waals interaction (Figure 4b).

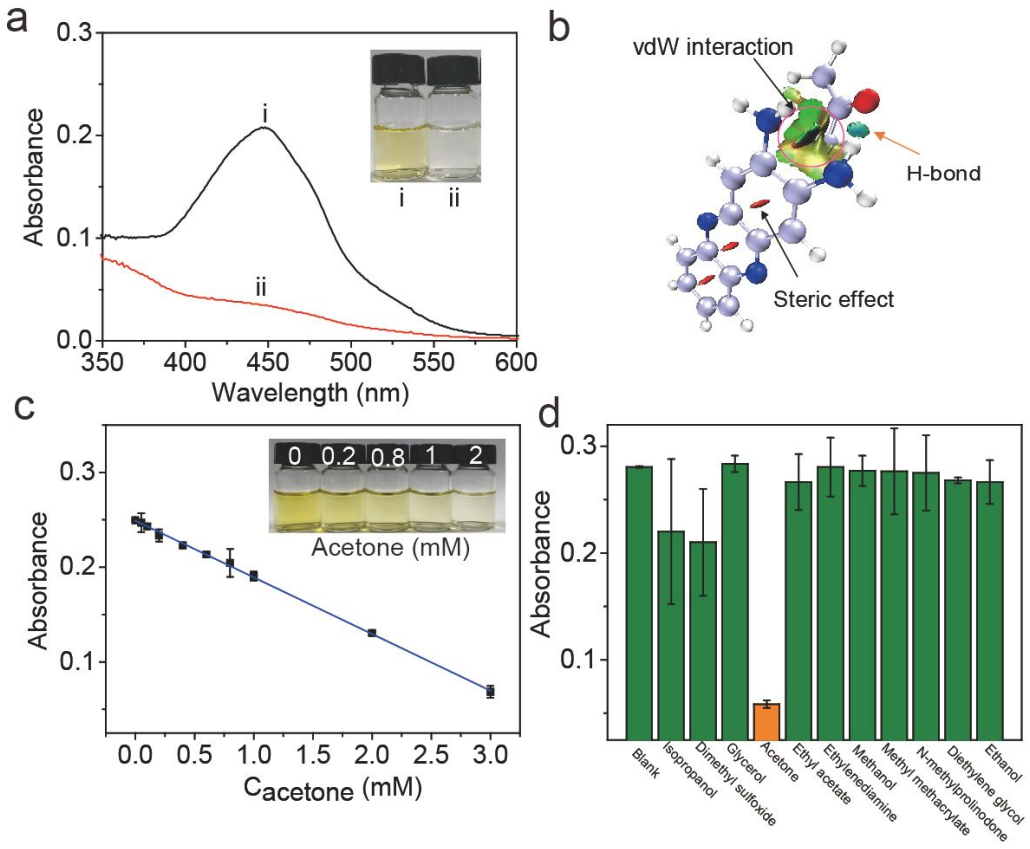

Figure 4. (a) Analytical performance for detection of acetone. UV-vis absorption spectra and the corresponding optical images of the exponential amplification chromogenic system in the absence and presence of 13 mM acetone. (b) Calculated interaction force between DAP and acetone in the complex of DAP · acetone. (c) Linear calibration curve for colorimetric detection of acetone. The inset shows the optical images of chromogenic system upon addition of different concentrations of acetone. (d) Selectivity evaluation for acetone detection. The concentration of acetone and all other common solvents is kept at 3 mM.

From the above-mentioned chromogenic reaction mechanism, the ISC process from S_1 to T_1 is the key step in the production of ·OH and Fe^{3+} cycle, and it is largely influenced by ΔE_{ST}. Generally, a small ΔE_{ST} value is favorable for the ISC process[40-42]. By calculating the energy levels of the singlet and triplet states, we can assess the ΔE_{ST} values, namely, 2.76 eV and 1.96 eV for DAP · acetone complex and DAP (Figure S11), respectively. Such an increase of ΔE_{ST} by approximately 41% should be

associated with the interaction between acetone and DAP, suppressing the ISC process and therefore leading to an extremely inefficient ·OH formation.

Benefiting from its acetone-response behavior, the cascade chromogenic system is applied for visual colorimetric detection of acetone. Varying concentrations of acetone from 0 to 3 mM were injected into the cascade chromogenic system, and the UV-vis absorption spectra are recorded at 15 min under blue-light LED illumination (Figure S12). With the increase of acetone concentration, the optical absorption of this cascade chromogenic system becomes gradually weak. A linear calibration curve is acquired from the absorbance values at 446 nm as a function of acetone concentration in the range of 50 μM-3 mM (Figure 4c). The limit of detection (LOD) is calculated to be 35 μM based on 3 σ/k, where σ and k are the standard deviation of the absorbance without acetone and slope of the linear calibration curve, respectively. This LOD is lower two to three order of magnitudes than that of the reported fluorescent assays[43-48]. The high sensitivity of this colorimetric assay is ascribed to the fact that the production of ·OH with high reaction activity is obviously restrained when the 1:1 DAP · acetone complex is generated (Figure S11). Fascinatingly more, the presence of acetone at a concentration of 1 mM can be observed with the naked eye due to the distinct color fading (the inset of Figure 4c). Likewise, the selectivity of this colorimetric assay is estimated with common solvents each at a concentration of 3 mM. It is clear that only acetone leads to a notable absorbance quenching, and colorimetric signal produced by other solvents is close to the background signal (Figure 4d), illustrating a good selectivity of the present colorimetric method in differentiating acetone from non-target analytes. The generation of 1:1 DAP · acetone complex with unique energy levels are responsible for the high selectivity of the present system.

Finally, to demonstrate its practical potential, the performance of this colorimetric assay in diluted real water samples is also tested. The 50-fold diluted real water samples, including lake water, pond water, and river water, are spiked with acetone at different concentrations (50 μM, 0.4 mM, and 2 mM). The spiked samples are analyzed by the present colorimetric assay, and the results are listed in Table 1. The scope of the recoveries for real water samples is from 90.6% to 100.7%, and the calculated relative

standard deviation is not more than 9%. The three concentrations of acetone are lower than the maximum limit level for environmental water set by U.S. Environmental Protection Agency (3.79 mM)[49]. These results prove the present colorimetric assay as a potential analytical technique for practical environmental monitoring. It should also be noted that this colorimetric assay can not be applied for direct detection of acetone in highly polluted water because the organic pollutants can not only influence the dissolved oxygen concentration, but also consume the ·OH. Some sample pretreatment techniques have to be performed before colorimetric detection of acetone using this colorimetric assay.

Table 1. Colorimetric detection results of acetone in real water samples

Samples	Added (mM)	Found (mM)	Recovery (%)	RSD (%)
Lake water	0.05	0.048	96.1	2.7
	0.4	0.38	94.6	8.1
	2	2.01	100.7	5.1
Pond water	0.05	0.047	94.9	1.8
	0.4	0.37	93.1	3
	2	1.99	99.3	7.2
River water	0.05	0.049	98.5	2.6
	0.4	0.39	99	2.8
	2	1.81	90.6	5.7

CONCLUSIONS

In conclusion, we have developed a cascade chromogenic system based on coupling chemical oxidation with photo-induced radical chain reaction. The high efficiency of Fe^{3+}-induced chemical oxidation and photo-induced Fenton-like reactions trigger an amplification process and generates an exponential colorimetric signal growth. By relying on the complex formation of DAP and acetone, this cascade chromogenic system is successfully utilized to visually determine acetone with a good selectivity over ten common solvents. The obtained sensitivity is two to three order of magnitudes better than that of the reported fluorescent assays. Of special note, the present colorimetric assay can be performed even in diluted real water samples. The resulting cascade chromogenic system features exceptional merits such as good accuracy, low

cost, easy operation, high portability, inexpensive instrumentation as well as high controllability, without the participation of enzymes or auto-inductive molecular receptors, which offers great prospects as a simple and reliable analytical method for in-field environmental monitoring. Meanwhile, by further coupling this cascade system with specific reactions or Fe^{3+}-involved nanomaterials, in principle, it is most likely to extend this chromogenic system to detect various desired analytes.

ASSOCIATED CONTENT

Supporting Information

The Supporting Information is available free of charge on the ACS Publications website at DOI:.

Calculation details, Mass spectrum, fluorescent emission spectrum, UV-vis absorption spectra and Energy level diagram (PDF)

AUTHOR INFORMATION

Corresponding Author

*E-mail: yhe2014@126.com

Notes

The authors declare no competing financial interest.

ACKNOWLEDGEMENTS

This work is supported by the Longshan Scholars Programme of Southwest University of Science and Technology (18LZX204) and China Aerodynamics Research and Development Center Foundation (Grant No. JPD20170142).

REFERENCES

(1) Nam, J. M.; Thaxton, C. S.; Mirkin, C. A. *Science* **2003**, *301*, 1884-1886.

(2) Liu, J.; Lu, Y. *J. Am. Chem. Soc.* **2003**, *125*, 6642-6643.

(3) Li, H.; Rothberg, L. *Proc. Natl. Acad. Sci. U. S. A.* **2004**, *101*, 14036-14039.

(4) De La Rica, R.; Stevens, M. M. *Nat. Nanotechnol.* **2012**, *7*, 821.

(5) Zhou, W.; Gao, X.; Liu, D.; Chen, X. *Chem. Rev.* **2015**, *115*, 10575-10636.

(6) Farka, Z.; Jurik, T.; Kovar, D.; Trnkova, L.; Skladal, P. *Chem. Rev.* **2017**, *117*, 9973-10042.

(7) Koide, K.; Tracey, M. P.; Bu, X.; Jo, J.; Williams, M. J.; Welch, C. J. *Nat. Commun.* **2016**, *7*, 10691.

(8) Nugroho, F. A.; Darmadi, I.; Cusinato, L.; Susarrey-Arce, A.; Schreuders, H.; Bannenberg, L. J.; Da Silva Fanta, A. B.; Kadkhodazadeh, S.; Wagner, J. B.; Antosiewicz, T. J. *Nat. Mater.* **2019**, *18*, 489.

(9) Li, R.; An, H.; Huang, W.; He, Y. *Sens. Actuators, B* **2018**, *259*, 59-63.

(10) Liu, W.; Xu, Q.; Cui, W.; Zhu, C.; Qi, Y. *Angew. Chem., Int. Ed.* **2017**, *56*, 1600-1604.

(11) Du, J.; Zhao, M.; Huang, W.; Deng, Y.; He, Y. *Anal. Bioanal. Chem.* **2018**, *410*, 4519-4526.

(12) Goertz, J. P.; White, I. M. *Angew. Chem., Int. Ed.* **2017**, *56*, 13411-13415.

(13) Sella, E.; Shabat, D. *J. Am. Chem. Soc.* **2009**, *131*, 9934-9936.

(14) Valentini, P.; Pompa, P. P. *Angew. Chem., Int. Ed.* **2016**, *55*, 2157-2160.

(15) Bi, S.; Yue, S.; Zhang, S. *Chem. Soc. Rev.* **2017**, *46*, 4281-4298.

(16) Yoon, H. J.; Mirkin, C. A. *J. Am. Chem. Soc.* **2008**, *130*, 11590-11591.

(17) Sun, X.; Dahlhauser, S. D.; Anslyn, E. V. *J. Am. Chem. Soc.* **2017**, *139*, 4635-4638.

(18) Sella, E.; Lubelski, A.; Klafter, J.; Shabat, D. *J. Am. Chem. Soc.* **2010**, *132*, 3945-3952.

(19) Yoshii, T.; Onogi, S.; Shigemitsu, H.; Hamachi, I. *J. Am. Chem. Soc.* **2015**, *137*, 3360-3365.

(20) Baker, M. S.; Phillips, S. T. *J. Am. Chem. Soc.* **2011**, *133*, 5170-5173.

(21) Sun, X.; Anslyn, E. V. *Angew. Chem., Int. Ed.* **2017**, *56*, 9522-9526.

(22) Gabrielli, L.; Mancin, F. *J. Org. Chem.* **2016**, *81*, 10715-10720.

(23) Gnaim, S.; Shabat, D. *J. Am. Chem. Soc.* **2017**, *139*, 10002-10008.

(24) Omar, A.; Habib, S.; Fawzy, I.; Ahmed, A.; Hassan, E. *Mansoura J. Forensic Med. Clin. Toxicol.* **2008**, *2*, 17-44.

(25) Jia, Q.; Ji, H.; Zhang, Y.; Chen, Y.; Sun, X.; Jin, Z. *J. Hazard. Mater.* **2014**, *276*, 262-270.

(26) Fornera, S.; Walde, P. *Anal. Biochem.* **2010**, *407*, 293-295.

(27) Yang, J.; Zhang, Y.; Zhang, L.; Wang, H.; Nie, J.; Qin, Z.; Li, J.; Xiao, W. *Chem. Commun.* **2017**, *53*, 7477-7480.

(28) Yang, X.; Wang, E. *Anal. Chem.* **2011**, *83*, 5005-5011.

(29) Sun, J.; Wang, B.; Zhao, X.; Li, Z. J.; Yang, X. *Anal. Chem.* **2016**, *88*, 1355-1361.

(30) Wang, J.; Li, H.; Cai, Y.; Wang, D.; Bian, L.; Dong, F.; Yu, H.; He, Y. *Anal. Chem.* **2019**, *91*, 6155-6161.

(31) Li, M.; Chong, Y.; Fu, P. P.; Xia, Q.; Croley, T. R.; Lo, Y. M.; Yin, J.-J. *J. Agric. Food Chem.* **2017**, *65*, 9893-9901.

(32) Fan, X.; Wang, Y.; Deng, L.; Li, L.; Zhang, X.; Wu, P. *Anal. Chem.* **2019**, *91*, 9407-9412.

(33) Zhang, J.; Wu, S.; Lu, X.; Wu, P.; Liu, J. *Nano. Lett.* **2019**, *19*, 3214-3220.

(34) Wang, H.; You, C.; Tan, Z. *Chem. Eng. J.* **2018**, *350*, 89-99.

(35) He, W.; Zhou, Y.-T.; Wamer, W. G.; Boudreau, M. D.; Yin, J. J. *Biomaterials* **2012**, *33*, 7547-7555.

(36) Bai, X.; Huang, Y.; Lu, M.; Yang, D. *Angew. Chem., Int. Ed.* **2017,** *56*, 12873-12877.

(37) Nawaz, H.; Tian, W.; Zhang, J.; Jia, R.; Chen, Z.; Zhang, J. *ACS Appl. Mater. Interfaces* **2018**, *10*, 2114-2121.

(38) Choe, Y. J.; Byun, J. Y.; Kim, S. H.; Kim, *J. Appl. Catal. B* **2018,** *233*, 272-280.

(39) Lu, T.; Chen, F. *J. Comput. Chem.* **2012**, *33*, 580-592.

(40) Wu, W.; Xu, S.; Qi, G.; Zhu, H.; Hu, F.; Liu, Z.; Zhang, D.; Liu, B. *Angew. Chem., Int. Ed.* **2019**, *58*, 3062-3066.

(41) Wang, H.; Jiang, S.; Chen, S.; Li, D.; Zhang, X.; Shao, W.; Sun, X.; Xie, J.; Zhao, Z.; Zhang, Q. *Adv. Mater.* **2016**, *28*, 6940-6945.

(42) Xu, S.; Wu, W.; Cai, X.; Zhang, C.-J.; Yuan, Y.; Liang, J.; Feng, G.; Manghnani, P.; Liu, B. *Chem. Commun.* **2017**, *53*, 8727-8730.

(43) Gao, X.; Xu, Z.; Liu, M.; Zhang, P. *J. Solid. State. Chem.* **2019**, *271*, 110-114.

(44) Hao, Z.; Yang, G.; Song, X.; Zhu, M.; Meng, X.; Zhao, S.; Song, S.; Zhang, H. *J. Mater. Chem. A* **2014**, *2*, 237-244.

(45) Ma, D.; Wang, W.; Li, Y.; Li, J.; Daiguebonne, C.; Calvez, G.; Guillou, O. *CrystEngComm* **2010**, *12*, 4372-4377.

(46) Pan, H.; Wang, S.; Dao, X.; Ni, Y. *Inorg. Chem.* **2018**, *57*, 1417-1425.

(47) Yang, Y.; Chen, L.; Jiang, F.; Wu, M.; Pang, J.; Wan, X.; Hong, M. *CrystEngComm* **2019**, *21*, 321-328.

(48) Zuo, H.; Li, Y.; Liao, Y. *ACS. ACS Appl. Mater. Interfaces* **2019**, *11*, 39201-39208.

(49) USEPA 1986. Integrated Risk Information System (IRIS database) chemical file for acetone (67-64-1).

For Table of Contents Only